

A non-accreting neutron star and δ Scuti candidate revealed by asteroseismological modelling and radial velocity measurements

PING LI,^{1,2} WEN-PING LIAO*,^{1,2} SHENG-BANG QIAN,³ LEI ZANG,³ FANGBIN MENG,^{1,2} AND FANGZHOU YAN³

¹*Yunnan Observatories, Chinese Academy of Sciences (CAS), 650216 Kunming, China*

²*University of Chinese Academy of Sciences, No.1 Yanqihu East Rd, Huairou District, Beijing, China 101408*

³*School of Physics and Astronomy, Yunnan University, Kunming 650091, China*

ABSTRACT

SZ Lyn is an astrometric binary consisting of a δ Scuti star and an unseen component. The two stars around each other in an almost circular orbit ($e=0.186$) with a period of about 3.32 years. We aim to explore the physical properties of the two components using the radial velocity method and asteroseismology. Our results show that the δ Scuti variable is a post-main sequence star with a helium core ($M_{\text{He}} = 0.1671_{-0.0045}^{+0.0028} M_{\odot}$ and $R_{\text{He}} = 0.1414_{-0.0020}^{+0.0035} R_{\odot}$) surrounded by a burning hydrogen shell; its fundamental parameters is accurately calculated to be $M=1.82_{-0.02}^{+0.04} M_{\odot}$, $R=2.91_{-0.02}^{+0.02} R_{\odot}$, $L=17.07_{-2.61}^{+1.28} L_{\odot}$, and $X_c=0.078_{-0.004}^{+0.021}$; the mass of the invisible object is thus estimated to be $M_{\text{co}}=1.68_{-0.60}^{+0.62} M_{\odot}$. Combined with the low-resolution LAMOST spectrum, we suggest that the unseen object is an neutron star candidate. Our work demonstrates the methodology of using the radial velocity method and asteroseismology to detect the compact object in such an astrometric binary.

Keywords: Astrometric binary (79) — Delta Scuti variable stars (370) — Asteroseismology(73) — Neutron stars(1108)

1. INTRODUCTION

Astrometric binary is a system where one star in the binary is significantly brighter than the other; it may not be possible to observe both stars directly, but the invisible star can be inferred by observing the oscillation of the visible star (Carroll & Ostlie 2017). The unseen star may be a neutron star (NS) or a white dwarf (WD). The mass distribution and physical properties of NSs contain important information about the history of stellar evolution and chemical enrichment in our Galaxy (Özel et al. 2012; Yi et al. 2022). NSs are usually found by different electromagnetic window (Keane & Kramer 2008), such as rapidly rotating and strongly magnetised radio pulsars (Lorimer 2008), accreting X-ray binaries, gamma-ray pulsars (Abdo et al. 2010), and nearby isolated thermally-emitting NSs (Haberl 2007). In addition, LIGO (Laser Interferometer Gravitational-wave Observatory) and Virgo can be used to detect merging NSs that produce gravitational waves (Abbott et al. 2017). However, if NSs are not beaming towards us, or if the NSs are not accreting material from their companions, then they cannot be detected by radio, X-ray or gamma-ray observations (Yi et al. 2022). Additionally, the population of non-accreting and/or radio-quiet NSs remains largely undetected (Caraveo et al. 1996).

The largest archival spectroscopic database of millions of stars has been provided by the Guoshoujing telescope (the Large-Sky Area Multi-Object Fibre Spectroscopic Telescope, LAMOST) (Cui et al. 2012; Zhao et al. 2012). By mining the wealth of large spectroscopic databases, the radial velocity (RV) method can be used to discover systems (Trimble & Thorne 1969) that host a hidden compact object orbiting around a luminous stellar companion: for example, stellar-mass black hole residing in wide binaries with an orbital period of typically ≥ 50 d, MWC 656 (Casares et al. 2014), LB-1 (Liu et al. 2019), J05215658+4359220 (Thompson et al. 2019). Surprisingly, this method could be used to search for NSs contained in binary systems, and many candidates had been found, such as J112306.9+400736 (Yi et al. 2022)

and V723 Monocerotis (Jayasinghe et al. 2021). By synergizing multi-epoch spectroscopic and photometric surveys, we can dynamically measure the masses of compact stars.

SZ Lyn (TIC 192939152) is an astrometric binary with an orbital period of about 3.32 years, containing a δ Scuti variable and an unseen body (Gazeas et al. 2004), at a distance of about 397 pc (Adassuriya et al. 2021). δ Scuti variables, on or near the main sequence evolutionary phase, are A- to F-type stars. They pulsate mainly in both radial and non-radial p modes, with some also exhibiting a low-order g mode, offering the potential to probe the stellar structure (Breger et al. 1993) and basic parameters such as stellar mass. Many δ Scuti stars have been observed by LAMOST, some of which have been found to be candidates for binary or multiple systems (Qian et al. 2018). SZ Lyn is also a single-lined spectroscopic binary (Bardin & Imbert 1984), and has been studied several times for its pulsation, for example the fundamental pulsation period for this star was first determined by Binnendijk (1968) and then refined by Gazeas et al. (2004). In recent years, Adassuriya et al. (2021) had reported four frequencies $f_1=8.296$ d^{-1} , $f_2=14.535$ d^{-1} , $f_3=32.620$ d^{-1} and $f_4=4.584$ d^{-1} , where f_1 , corresponding to the main pulsation period, is a radial p mode with the largest amplitude; f_2 , f_3 and f_4 are first detected by them and identified as two non-radial lower order p modes and a candidate of g mode. The δ Scuti star has both p and g modes, making it a good target for asteroseismic modelling to estimate its physical properties such as mass, luminosity and radius, etc. The physical properties of the faint companion will then be further investigated.

2. RADIAL VELOCITY ANALYSIS

Figure 1 shows a low-resolution spectrum of SZ Lyn, which was taken from DR7 of LAMOST low-resolution single-epoch spectra (Bai et al. 2021). By fitting the full spectrum to mode spectra generated by an interpolator using the ELODIE library (Prugniel & Soubiran 2001), the University of Lyon Spectroscopic Analysis Software (ULySS) (Koleva et al. 2009) was then used to obtain stellar atmospheric parameters. Then they were determined to be $T_{\text{eff}}=7173$ (± 146) K, $\log g=3.87$ (± 0.01), $[Fe/H]=-0.08$ (± 0.01). In order to measure the radial velocity (RV) with respect to

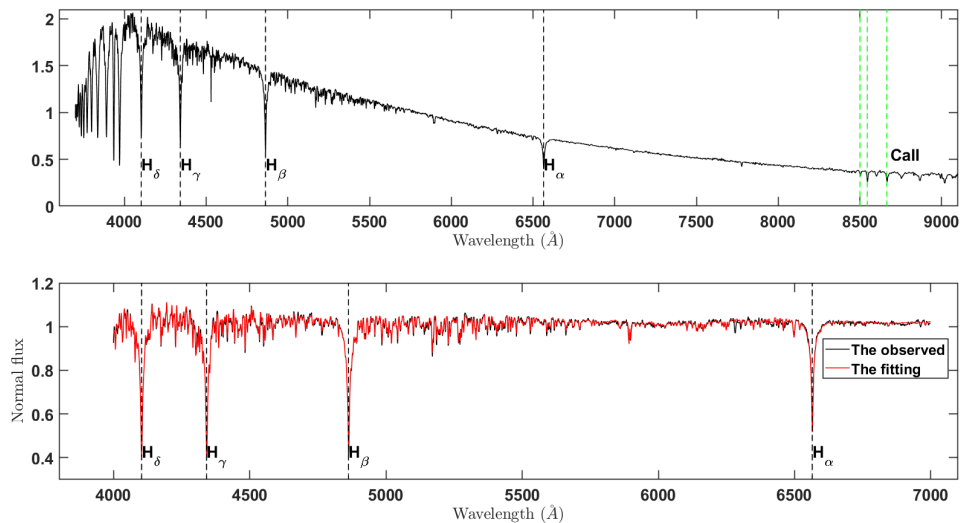


Figure 1. The low-resolution spectrum of SZ Lyn observed with LAMOST. Upper panel: The original spectrum, the four Balmer absorbed lines H_α , H_β , H_γ , and H_δ and the metal lines CaII are marked. Lower panel: The fitting model of A-type star for the spectrum of SZ Lyn.

the heliocentric frame of reference, we use the cross-corresponding function (CCF) method to process the absorption line of SZ Lyn, then the CCF profile are fitted by using the Gaussian function. The value of RV thus is estimated to be 32 (± 4) (km/s). We also collected 21 RV values from Bardin & Imbert (1984), covering one orbital period of SZ Lyn.

The following equations (Iglesias-Marzoa et al. 2015) are used to fit the RV values

$$V_r = \gamma + K[\cos(\theta + \omega) + e \cos(\omega)], \quad (1)$$

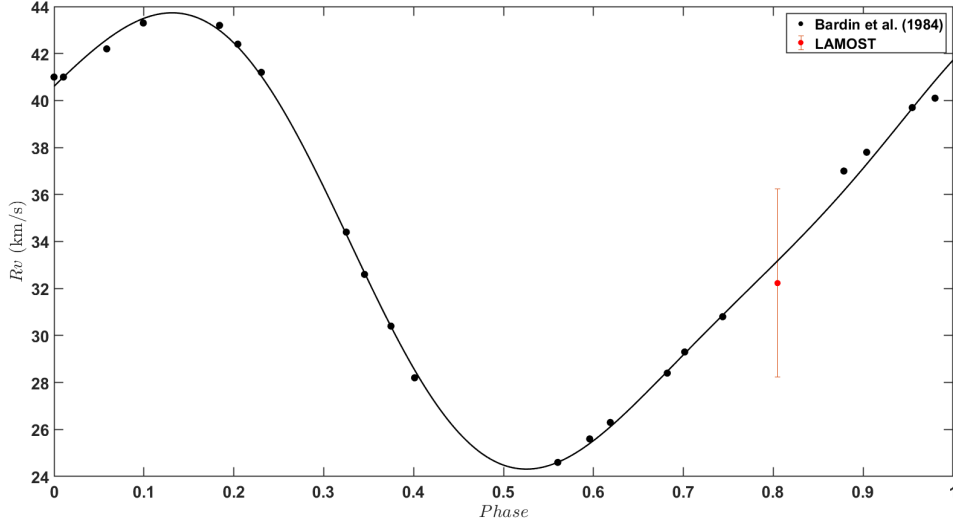


Figure 2. The radial velocity curve of SZ lyn.

$$\theta(t) = 2 \arctan\left[\sqrt{\frac{1+e}{1-e}} \tan\left(\frac{E}{2}\right)\right], \quad (2)$$

$$E - e \sin(E) = \frac{2\pi}{P}(t - T_p), \quad (3)$$

where γ , K , ω , e , E , P , and T_p are the center of mass velocity of binary system, the semi-amplitude of RV, the eccentricity of the orbit, the eccentric anomaly, the orbital period of binary system, and the time of periastron passage, respectively.

As shown in Figure 2, by fitting the RV values, these parameters are estimated to be $\gamma=34.18 (\pm 0.05)$ (km/s), $K=9.51 (\pm 0.09)$ (km/s), $\omega=101.2 (\pm 1.4)^\circ$, $e=0.186 (\pm 0.009)$, $P=1188.51 (\pm 7.59)$ days and $T_p=2452751.81 (\pm 19.13)$, respectively. Then we obtain the value of mass function is

$$f(m) = \frac{M_{co}^3 \sin^3(i)}{(M + M_{co})^2} = 10361 \times 10^{-7} (1 - e^2)^{3/2} K^3 P M_\odot = 0.1005 (\pm 0.003) M_\odot. \quad (4)$$

where M , M_{co} and i are the masses of the δ Scuti star and the invisible component, and the inclination of the orbit, respectively.

3. STELLAR MODEL AND ASTEROSEISMIC ANALYSIS FOR δ SCUTI

3.1. Input Physics

The Modules for Experiments in Stellar Astrophysics (MESA, r22.11.1) stellar evolution code, developed by Paxton et al. (2011, 2013, 2015, 2018), is used to compute evolution and pulsation models. In particular, the "pulse-adipls" submodule in MESA is used to compute the adiabatic frequencies of radial or non-radial p and non-radial g modes (Christensen-Dalsgaard 2008). The OPAL opacity tables from Iglesias & Rogers (1996) are used for the high temperature zone, and Ferguson et al. (2005) for the low temperature zone. It is assumed that the initial component of metallicity is identical to that of the Sun (Asplund et al. 2009). The classical mixing length theory (Böhm-Vitense 1958) with $\alpha=1.90$ (Paxton et al. 2011) is used in the convective zone. In addition, we adopt an exponentially decaying prescription and introduce an overshooting mixing diffusion coefficient (Freytag et al. 1996; Herwig 2000) for the overshooting mixing of the convective core.

$$D_{ov} = D_0 \exp\left(\frac{-2z}{f_{ov} H_p}\right), \quad (5)$$

where D_0 indicates the diffusion mixing coefficient near the edge of the convective core, z is the distance into the radiative zone away from the edge, f_{ov} is the efficiency of the overshooting mixing, and H_p is the pressure scale height. The lower limit of the diffusion coefficient is set to $D_{\text{ov}}^{\text{limit}} = 1 \times 10^{-2} \text{ cm}^2 \text{ s}^{-1}$, below which the overshooting is turned off. Finally, elemental diffusion and magnetic fields on stellar structure and evolution are not included in this work.

3.2. Grid of Stellar Models

In our models, a star's evolutionary path and internal structure depend on its initial mass M , chemical composition (X, Y, Z) and overshooting parameter f_{ov} . Following the method of Li et al. (2018), the initial helium abundance is set to $Y = 0.249 + 1.33Z$, allowing the evolution and structure of the star to be completely determined by the values of M , Z and f_{ov} . The grid search of stellar mass M is set between $1.70 M_{\odot}$ and $2.0 M_{\odot}$ with a step of $0.01 M_{\odot}$, and the fraction of metallicity $[Fe/H]$ is set in the range of -0.090 to -0.070 with steps of -0.002 . The relationship of Fe/H and Z is defined by

$$[Fe/H] = \log\left(\frac{Z}{X}\right) + \log\left(\frac{Z}{X}\right)_{\odot}, \quad (6)$$

where we use the value of $(Z/X)_{\odot} = 0.0181$ (Asplund et al. 2009). For the overshooting mixing, we consider four different cases: no overshooting ($f_{\text{ov}} = 0$), moderate overshooting ($f_{\text{ov}} = 0.01$), intermediate overshooting ($f_{\text{ov}} = 0.02$) and extreme overshooting ($f_{\text{ov}} = 0.03$). We also take into account the rotation of the δ Scuti star, its surface velocity is set at 10 km/s (Adassuriya et al. 2024). According to the spectroscopic observations of LAMOST, The δ Scuti is an A6 type star with an effective temperature of about 7173 K , and thus the corresponding effective temperature constraint is set to $6673 \text{ K} < T_{\text{eff}} < 7673 \text{ K}$ with a range of 500 K (Chen et al. 2020). From the zero-age main sequence to the post-main sequence, each star in the grid is calculated. For theoretical models that satisfy the constraint, we estimate their frequencies of radial oscillations ($l=0$) and non-radial oscillations with $l=1$ and $l=2$.

3.3. Grid of Stellar Models

In order to find the best model to observations, we compare model frequencies with the observed frequencies f_1 , f_2 , f_3 , and f_4 according to

$$S^2 = \frac{1}{k} \sum (|f_{\text{model},i} - f_{\text{obs},i}|^2), \quad (7)$$

where $f_{\text{obs},i}$ indicates the observed frequency, $f_{\text{model},i}$ represents its corresponding theoretical model frequency, and k is the number of observed frequencies. In our calculations, the theoretical model frequencies nearest to the above frequencies f_1 , f_2 , f_3 , and f_4 are regarded as their possible model counterparts.

Figures 3 and 4 show plots of resulting S_m^2 versus different stellar fundamental parameters. Figure 3 (a) shows variations of S_m^2 as a function of the stellar mass M . We found that the values of M cover a good range of $1.80 M_{\odot}$ - $1.86 M_{\odot}$, while the stellar masses of theoretical models with two overshooting mixing show excellent convergence, i.e., $1.80 M_{\odot}$ - $1.86 M_{\odot}$ for $f_{\text{ov}}=0.01$ and $1.72 M_{\odot}$ for $f_{\text{ov}}=0.00$. Because there is only one convergent result with good S_m^2 for $f_{\text{ov}}=0.00$, and its S_m^2 larger than the S_m^2 of $f_{\text{ov}}=0.01$, so we don't consider it in this work. Figure 3 (b) shows variations of S_m^2 as a function of the stellar luminosity L , values of L are found to cover a wide range, i.e., $15.46 L_{\odot}$ - $18.35 L_{\odot}$. Figure 3 (c) and (d) show changes of S_m^2 as a function of the stellar radius R and the effective temperature T_{eff} , we found that the values of R converge well to $2.89 R_{\odot}$ - $2.93 R_{\odot}$ and those of T_{eff} converge well to 6727 K - 6978 K .

Figure 4 (a)-(c) present changes of S_m^2 as a function of the initial metallicity $[Fe/H]$, the mass of helium core M_{He} , and the radius of the helium core R_{He} . It can be clearly seen that the values of $[Fe/H]$ cover -0.090 - -0.070 , the values of M_{He} converge well to $0.1626 M_{\odot}$ - $0.1699 M_{\odot}$, and those of R_{He} are distributed in a narrow range of $0.1394 R_{\odot}$ - $0.144 R_{\odot}$. Figure 4 (d)-(f) show changes of S_m^2 as a function of the gravitational acceleration $\log g$, the mass fraction of central hydrogen X_c , and the age of star. We found that the values of $\log g$ are distributed in a narrow range of 3.770 - 3.776 , the values of X_c converge well to 0.074 - 0.099 , and those of Age converge to 1.15×10^9 years- 1.25×10^9 years. In addition, as shown in 3 and 4, the best-fitting model has a moderate overshooting ($f_{\text{ov}}=0.10$).

Based on the above calculations, the basic parameters of the δ Scuti star obtained from the asteroseismic models are listed in Table 1. The comparisons between observed and model frequencies are listed in Table 2. According to the comparisons, f_1 is identified as a radial p-mode of the first overtone, f_2 is identified as a quadrupole f-mode, f_3 is not produced in our asteroseismic model and f_4 is detected as a non-radial g-model with $l=3$.

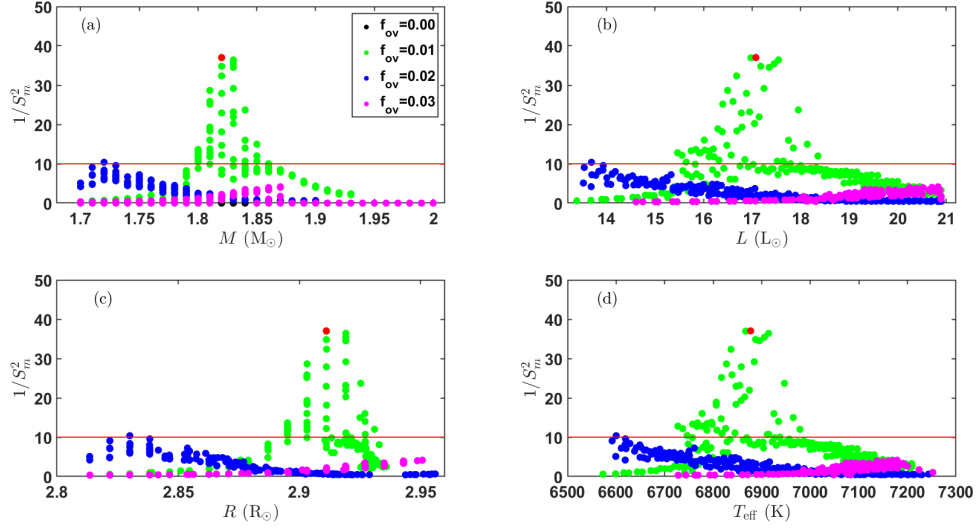


Figure 3. Visualization of fitting results S_m^2 and stellar basic parameters: the stellar mass M , the luminosity L , the radius R , and the effective temperature T_{eff} , respectively. Each dot represents one minimum value of S^2 along one evolutionary track of star. The dots in black, green, blue, and pink correspond to theoretical models with $f_{\text{ov}}=0, 0.10, 0.20$, and 0.03 , respectively. The red horizontal line marks the position of $S_m^2 = 0.1$, which corresponds to the square of the frequency resolution $1/\Delta T$, where ΔT is the continuous observation time of one sector of the TESS (the Transiting Exoplanet Survey Satellite). The dots above the horizontal line correspond to 45 candidate models, while the red dot corresponds to the best-fitting model.

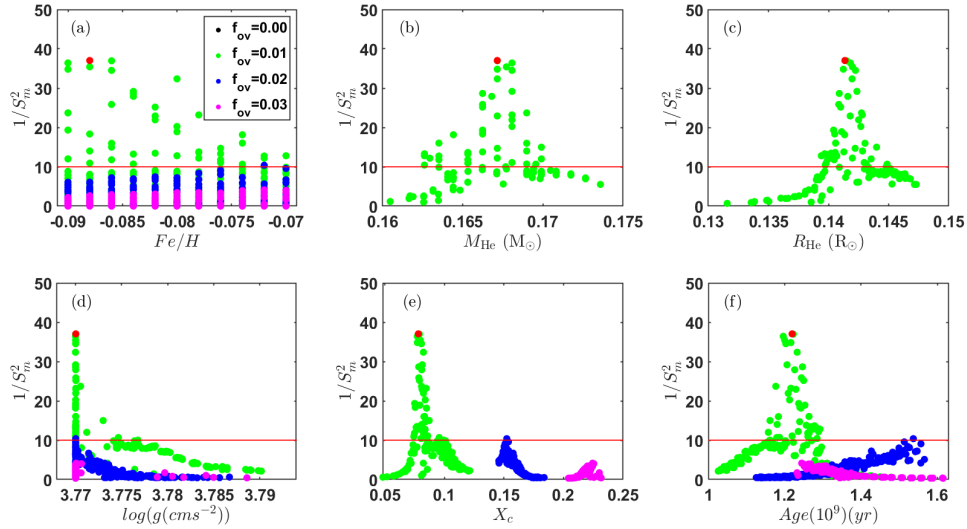


Figure 4. Visualization of fitting results S_m^2 and stellar basic parameters: the initial metallicity $[Fe/H]$, the mass of helium core M_{He} , the radius of helium core R_{He} , the gravitational acceleration $\log g$, the mass fraction of central hydrogen X_c , and the age of star, respectively. Each dot represents one minimum value of S^2 along one evolutionary track of star. The dots in black, green, blue and pink correspond to theoretical models with $f_{\text{ov}}=0, 0.10, 0.20$ and 0.03 , respectively. The red horizontal line marks the position of $S_m^2 = 0.1$, which corresponds to the square of the frequency resolution $1/\Delta T$, where ΔT is the continuous observation time of one sector of the TESS. The dots above the horizontal line correspond to 56 candidate models, while the red dot corresponds to the best-fitting model.

Figure 5 shows the position and evolutionary track of the δ Scuti star of the best-fitting model on the Hertzsprung-Russell (H-R) diagram. This means the δ Scuti component is a post-main sequence star with age about 1.21×10^9 years. When the star is in this position, the three frequencies (f_1 , f_2 and f_4) can be produced synchronously and are

Table 1. Fundamental parameters of SZ Lyn. The data in brackets are the values of the best fitting model, the upper and lower uncertainties are calculated using the maximum and minimum values of the candidate models minus those values in the brackets.

Parameters	values
M (M_{\odot})	1.80-1.86 (1.82 $^{+0.04}_{-0.02}$)
T_{eff} (K)	6727-6978(6877 $^{+149}_{-101}$)
$\log g$	3.77-3.776 (3.77 $^{+0.006}_{-0.000}$)
R (R_{\odot})	2.89-2.93 (2.91 $^{+0.02}_{-0.02}$)
L (L_{\odot})	15.46-18.35 (17.07 $^{+1.28}_{-2.61}$)
X_c	0.074-0.099 (0.078 $^{+0.021}_{-0.004}$)
M_{He} (M_{\odot})	0.1626-0.1699 (0.1671 $^{+0.0028}_{-0.0045}$)
R_{He} (R_{\odot})	0.1394-0.1449 (0.1414 $^{+0.0035}_{-0.0020}$)
Age (10^9 yr)	1.15-1.29 (1.21 $^{+0.08}_{-0.06}$)
[Fe/H]	-0.09- -0.070 (-0.088 $^{+0.002}_{-0.018}$)
f_{ov}	0.01

Table 2. Comparison between observed and model frequencies of the best-fitting model. f_{ob} is the observed frequency and f_{mod} is the model frequency. (n, m, l) are the radial order, the azimuthal number of the model frequency, and the spherical harmonic degree, respectively. $|f_{\text{ob}} - f_{\text{mod}}|$ indicates the frequency difference between the observed frequency and its model counterpart. $\beta_{1,n}$ is rotational parameter (Aerts et al. 2010).

ID	f_{ob} (μHz)	f_{mod} (μHz)	(n, m, l)	$\beta_{1,n}$	$ f_{\text{ob}} - f_{\text{mod}} $
f_1	96.0185	96.3689	(1, 0, 0)	0.916	0.3504
f_2	168.2291	168.4574	(0, 1, 2)	0.916	0.2283
f_3	377.5462
f_4	53.0555	53.1738	(-15, 1, 3)	0.416	0.1183

close to the corresponding observed frequencies. This indicates that the theoretical model and the actual structure of the δ Scuti star are nearly alike. In addition, the fraction of central hydrogen is estimated to be $X_c=0.078^{+0.021}_{-0.004}$, which means that the δ Scuti star has a convective helium core that surrounded by a burning hydrogen shell. Thus the size of helium core of the δ Scuti component is calculated to be $M_{\text{He}}=0.1671^{+0.0028}_{-0.0045} M_{\odot}$ and $R_{\text{He}}=0.1414^{+0.0035}_{-0.0020} R_{\odot}$.

4. DISCUSSIONS AND CONCLUSIONS

SZ Lyn is an astrometric binary system that contains a δ Scuti variable and an invisible component. They orbit around each other in a nearly circular orbit ($e=0.186$) with an orbital period of about 3.25 years. Using the astrometric data from the Hipparcos mission, the value of orbital inclination i is determined to be $39.5 (\pm 17.7)^{\circ}$ (Li & Qian 2013). We model the δ Scuti star using MESA code and three pulsating frequencies are well estimated. Thus the exact fundamental parameters of the δ Scuti star are calculated to be $M=1.82^{+0.04}_{-0.02} M_{\odot}$, $R=2.91^{+0.02}_{-0.02} R_{\odot}$ and $L=17.07^{+1.28}_{-2.61} L_{\odot}$. The frequency f_3 may have more complicated physical causes and requires a more complex model to estimate. Therefore, the mass of the invisible star then is calculated to be $M_{\text{co}}=1.68^{+0.62}_{-0.60} M_{\odot}$ using mass function (4). According to Kepler's third law, the separation between the two components is $a=3.33^{+0.04}_{-0.03}$ au, where au is the astronomical unit. This measured mass indicates that the unseen component is either a massive WD or an NS, since normal stars of similar mass are easily detected by spectroscopic method. The Roche lobe filling factor of the δ star is $f=R/R_L \approx 0.0068$, where R_L is the radius of Roche lobe. Therefore, the component cannot accrete mass from the δ Scuti variable, so it could not be observed in X-ray or gamma-ray.

As shown in the upper panel of Figure 1, the four Balmer and the CaII absorbed lines are apparent. Also, the Balmer absorbed lines are well fitted with A-type star. Indeed, in our work and the previous studies (Bardin & Imbert

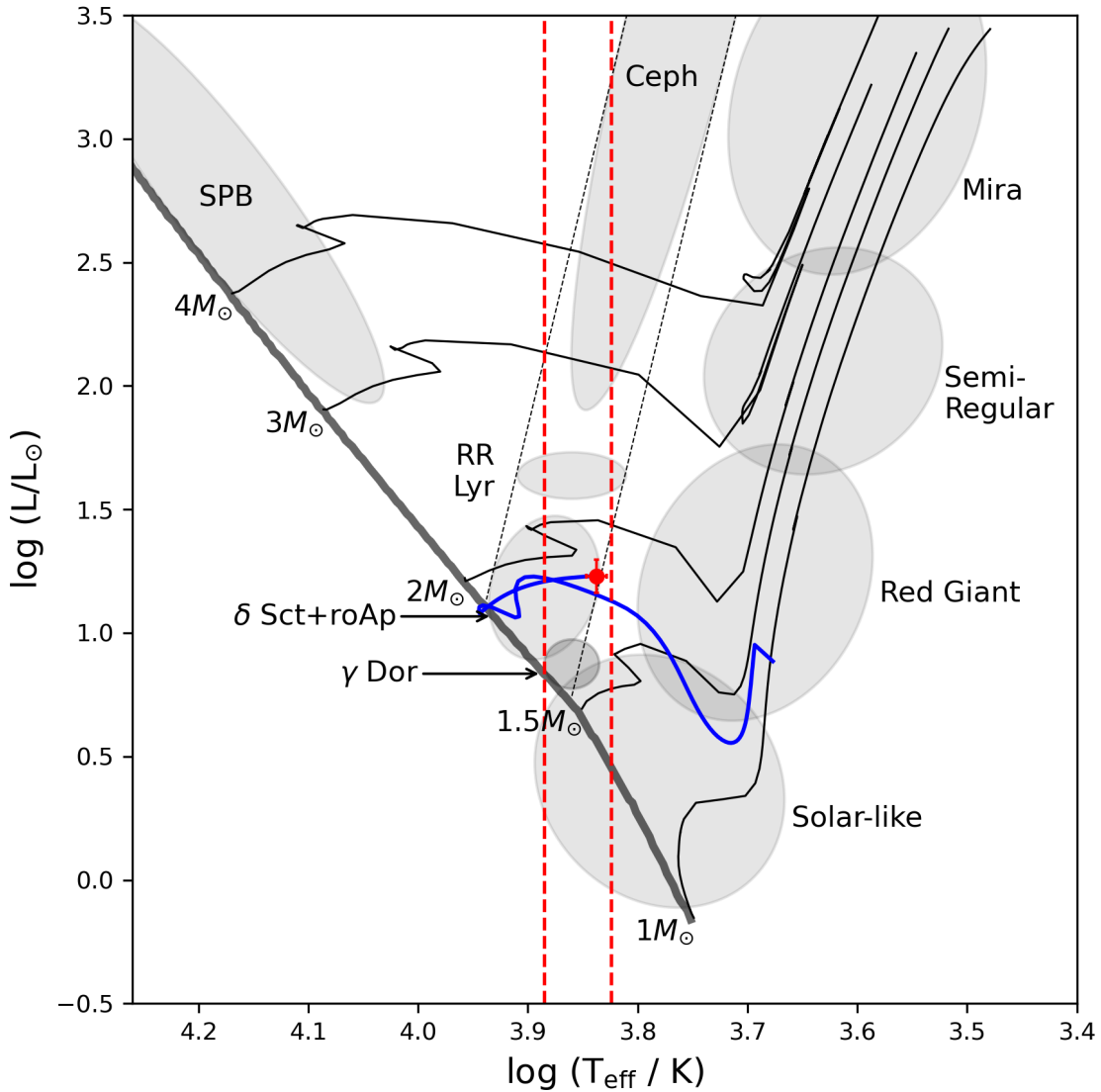


Figure 5. The location of SZ lyn in Hertzsprung-Russell (H-R) diagram. The vertical dash lines mark the location of 6673 $K < T_{\text{eff}} < 7673$ K. The blue solid line shows the evolutionary trajectory of SZ lyn from the pre-main sequence stage to the post-main sequence stage ($M=1.82 M_{\odot}$, $f_{\text{ov}}=0.01$, $[Fe/H]=-0.088$).

1984; Gazeas et al. 2004), no any emission line is found that moves in antiphase to the δ Scuti motion if it comes from the compact object's side. Additionally, we suggested that the invisible component is an Ns. However, the possibility that the invisible component is a WD cannot be completely ruled out if the compact body is a massive WD with a low effective surface temperature ($\leq 10^4$ K) and small size, causing it to contribute less luminosity, because the δ Scuti is absolutely dominant on spectra. Therefore, it can be easily neglected by traditional WD surveys.

The invisible star in some astrometric binary system can be revealed from its hidden side by the RV measurement, astrometry and asteroseismology supported by optical time domain surveys. Our work shows that such an astrometric binary SZ Lyn contains a NS candidate, using the method of RV curve measurement and asteroseismological modelling. But the inclination of the orbit in our work is not precise enough, and it lacks the evidence of the radio observations. However, Gaia's precise astrometry is also capable of finding hidden BHs, NSs, WDs, for example Gaia BH3 (Balbinot et al. 2024). Indeed, the Five-hundred-meter Aperture Spherical radio Telescope (FAST) is an advanced telescope for searching NSs. Therefore, SZ Lyn needs to be observed further by such telescopes to investigate the NS candidate in the future.

This work is supported by the International Cooperation Projects of (No. 2022YFE0127300) the National Key R&D Program, the National Natural Science Foundation of China (No. 11933008), the Young Talent Project of “Yunnan Revitalization Talent Support Program” in Yunnan Province, the basic research project of Yunnan Province (Grant No. 202201AT070092), CAS “Light of West China” Program. This work has made use of data from the European Space Agency (ESA) mission Gaia. Processed by the Gaia Data Processing and Analysis Consortium. Funding for the DPAC has been provided by national institutions, in particular the institutions participating in the *Gaia* Multilateral Agreement. The TESS data presented in this paper were obtained from the Mikulski Archive for Space Telescopes (MAST) at the Space Telescope Science Institute (STScI). STScI is operated by the Association of Universities for Research in Astronomy, Inc. Support to MAST for these data is provided by the NASA Office of Space Science. Funding for the TESS mission is provided by the NASA Explorer Program.

APPENDIX

A. APPENDIX INFORMATION

REFERENCES

- Abbott, B. P., Abbott, R., Abbott, T. D., et al. 2017, *PhRvL*, 119, 161101, doi: [10.1103/PhysRevLett.119.161101](https://doi.org/10.1103/PhysRevLett.119.161101)
- Abdo, A. A., Ackermann, M., Ajello, M., et al. 2010, *ApJS*, 187, 460, doi: [10.1088/0067-0049/187/2/460](https://doi.org/10.1088/0067-0049/187/2/460)
- Adassuriya, J., Ganesh, S., De Cat, P., Joshi, S., & Jayaratne, C. 2024, *Bulletin de la Societe Royale des Sciences de Liege*, 93, 470, doi: [10.25518/0037-9565.11753OTHER:https://poppers.uliege.be/0037-9565/index.php?id=11753](https://doi.org/10.25518/0037-9565.11753OTHER:https://poppers.uliege.be/0037-9565/index.php?id=11753)
- Adassuriya, J., Ganesh, S., Gutiérrez, J. L., et al. 2021, *MNRAS*, 502, 541, doi: [10.1093/mnras/staa3923](https://doi.org/10.1093/mnras/staa3923)
- Aerts, C., Christensen-Dalsgaard, J., & Kurtz, D. W. 2010, *Asteroseismology*, doi: [10.1007/978-1-4020-5803-5](https://doi.org/10.1007/978-1-4020-5803-5)
- Asplund, M., Grevesse, N., Sauval, A. J., & Scott, P. 2009, *ARA&A*, 47, 481, doi: [10.1146/annurev.astro.46.060407.145222](https://doi.org/10.1146/annurev.astro.46.060407.145222)
- Bai, Z.-R., Zhang, H.-T., Yuan, H.-L., et al. 2021, *Research in Astronomy and Astrophysics*, 21, 249, doi: [10.1088/1674-4527/21/10/249](https://doi.org/10.1088/1674-4527/21/10/249)
- Balbinot, E., Dodd, E., Matsuno, T., et al. 2024, arXiv e-prints, arXiv:2404.11604, doi: [10.48550/arXiv.2404.11604](https://doi.org/10.48550/arXiv.2404.11604)
- Bardin, C., & Imbert, M. 1984, *A&AS*, 57, 249
- Binnendijk, L. 1968, *AJ*, 73, 29, doi: [10.1086/110591](https://doi.org/10.1086/110591)
- Böhm-Vitense, E. 1958, *ZA*, 46, 108
- Breger, M., Stich, J., Garrido, R., et al. 1993, *A&A*, 271, 482
- Caraveo, P. A., Bignami, G. F., & Trümper, J. E. 1996, *A&A Rv*, 7, 209, doi: [10.1007/s001590050004](https://doi.org/10.1007/s001590050004)
- Carroll, B. W., & Ostlie, D. A. 2017, *An introduction to modern astrophysics*, Second Edition
- Casares, J., Negueruela, I., Ribó, M., et al. 2014, *Nature*, 505, 378, doi: [10.1038/nature12916](https://doi.org/10.1038/nature12916)
- Chen, X., Zhang, X., Li, Y., et al. 2020, *ApJ*, 895, 136, doi: [10.3847/1538-4357/ab8bd2](https://doi.org/10.3847/1538-4357/ab8bd2)
- Christensen-Dalsgaard, J. 2008, *Ap&SS*, 316, 113, doi: [10.1007/s10509-007-9689-z](https://doi.org/10.1007/s10509-007-9689-z)
- Cui, X.-Q., Zhao, Y.-H., Chu, Y.-Q., et al. 2012, *Research in Astronomy and Astrophysics*, 12, 1197, doi: [10.1088/1674-4527/12/9/003](https://doi.org/10.1088/1674-4527/12/9/003)
- Ferguson, J. W., Alexander, D. R., Allard, F., et al. 2005, *ApJ*, 623, 585, doi: [10.1086/428642](https://doi.org/10.1086/428642)
- Freytag, B., Ludwig, H. G., & Steffen, M. 1996, *A&A*, 313, 497
- Gazeas, K. D., Niarchos, P. G., & Boutsia, K. A. 2004, *Communications in Asteroseismology*, 144, 26
- Haberl, F. 2007, *Ap&SS*, 308, 181, doi: [10.1007/s10509-007-9342-x](https://doi.org/10.1007/s10509-007-9342-x)
- Herwig, F. 2000, *A&A*, 360, 952, doi: [10.48550/arXiv.astro-ph/0007139](https://doi.org/10.48550/arXiv.astro-ph/0007139)
- Iglesias, C. A., & Rogers, F. J. 1996, *ApJ*, 464, 943, doi: [10.1086/177381](https://doi.org/10.1086/177381)
- Iglesias-Marzoa, R., López-Morales, M., & Jesús Arévalo Morales, M. 2015, *PASP*, 127, 567, doi: [10.1086/682056](https://doi.org/10.1086/682056)
- Jayasinghe, T., Stanek, K. Z., Thompson, T. A., et al. 2021, *MNRAS*, 504, 2577, doi: [10.1093/mnras/stab907](https://doi.org/10.1093/mnras/stab907)
- Keane, E. F., & Kramer, M. 2008, *MNRAS*, 391, 2009, doi: [10.1111/j.1365-2966.2008.14045.x](https://doi.org/10.1111/j.1365-2966.2008.14045.x)
- Koleva, M., Prugniel, P., Bouchard, A., & Wu, Y. 2009, *A&A*, 501, 1269, doi: [10.1051/0004-6361/200811467](https://doi.org/10.1051/0004-6361/200811467)

- Li, L.-J., & Qian, S.-B. 2013, PASJ, 65, 116, doi: [10.1093/pasj/65.6.116](https://doi.org/10.1093/pasj/65.6.116)
- Li, T., Bedding, T. R., Huber, D., et al. 2018, MNRAS, 475, 981, doi: [10.1093/mnras/stx3079](https://doi.org/10.1093/mnras/stx3079)
- Liu, J., Zhang, H., Howard, A. W., et al. 2019, Nature, 575, 618, doi: [10.1038/s41586-019-1766-2](https://doi.org/10.1038/s41586-019-1766-2)
- Lorimer, D. R. 2008, Living Reviews in Relativity, 11, 8, doi: [10.12942/lrr-2008-8](https://doi.org/10.12942/lrr-2008-8)
- Özel, F., Psaltis, D., Narayan, R., & Santos Villarreal, A. 2012, ApJ, 757, 55, doi: [10.1088/0004-637X/757/1/55](https://doi.org/10.1088/0004-637X/757/1/55)
- Paxton, B., Bildsten, L., Dotter, A., et al. 2011, ApJS, 192, 3, doi: [10.1088/0067-0049/192/1/3](https://doi.org/10.1088/0067-0049/192/1/3)
- Paxton, B., Cantiello, M., Arras, P., et al. 2013, ApJS, 208, 4, doi: [10.1088/0067-0049/208/1/4](https://doi.org/10.1088/0067-0049/208/1/4)
- Paxton, B., Marchant, P., Schwab, J., et al. 2015, ApJS, 220, 15, doi: [10.1088/0067-0049/220/1/15](https://doi.org/10.1088/0067-0049/220/1/15)
- Paxton, B., Schwab, J., Bauer, E. B., et al. 2018, ApJS, 234, 34, doi: [10.3847/1538-4365/aaa5a8](https://doi.org/10.3847/1538-4365/aaa5a8)
- Prugniel, P., & Soubiran, C. 2001, A&A, 369, 1048, doi: [10.1051/0004-6361:20010163](https://doi.org/10.1051/0004-6361:20010163)
- Qian, S. B., Li, L. J., He, J. J., et al. 2018, MNRAS, 475, 478, doi: [10.1093/mnras/stx3185](https://doi.org/10.1093/mnras/stx3185)
- Thompson, T. A., Kochanek, C. S., Stanek, K. Z., et al. 2019, Science, 366, 637, doi: [10.1126/science.aau4005](https://doi.org/10.1126/science.aau4005)
- Trimble, V. L., & Thorne, K. S. 1969, ApJ, 156, 1013, doi: [10.1086/150032](https://doi.org/10.1086/150032)
- Yi, T., Gu, W.-M., Zhang, Z.-X., et al. 2022, Nature Astronomy, 6, 1203, doi: [10.1038/s41550-022-01766-0](https://doi.org/10.1038/s41550-022-01766-0)
- Zhao, G., Zhao, Y.-H., Chu, Y.-Q., Jing, Y.-P., & Deng, L.-C. 2012, Research in Astronomy and Astrophysics, 12, 723, doi: [10.1088/1674-4527/12/7/002](https://doi.org/10.1088/1674-4527/12/7/002)